

RESERVOIR ENGINEERING OF **SHALLOW** FAULT-CHARGED HYDROTHERMAL SYSTEMS

S.M. Benson, G.S. Bodvarsson, and D.C. Mangold

Earth Sciences Division  
Lawrence Berkeley Laboratory  
Berkeley, California 94720

Introduction Many of the low-to-moderate temperature (< 150°C) hydrothermal resources being developed in the United States occur in near-surface aquifers. These shallow thermal anomalies, typical of the Basin and Range and Cascades are attributed to hydrothermal circulation. The aquifers are often associated with faults, fractures, and highly complex geological settings; they are often very limited in size and display anomalous temperature reversals with depth. Because of the shallow depth and often very warm temperatures of these resources, they are attractive for development of direct-use hydrothermal energy projects. However, development of the resources is hindered by their complexity, the often limited manifestation of the resource, and lack of established reservoir engineering and assessment methodology.

In this paper a conceptual model of these systems is postulated, a computational model is developed, and reservoir engineering methods (including reservoir longevity, pressure transient analysis, and well siting) are reevaluated to include the reservoir dynamics necessary to explain such systems. Finally, the techniques are applied to the Susanville, California hydrothermal anomaly.

Thermal Model Figure 1 shows a schematic of the conceptual model developed to explain the occurrence of near-surface hot water aquifers.

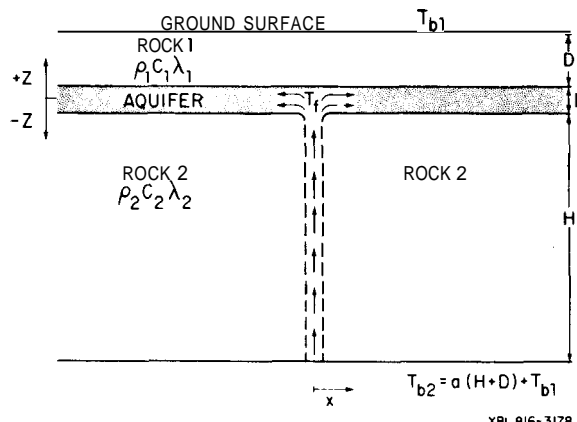


Figure 1 Schematic of a conceptual model for a fault-charged hydrothermal system.

Heated fluids rise along a fault until a highly permeable aquifer is intersected. Fluid then enters the aquifer and with time, replaces the existing fluid with hot water. As the water moves away from the fault it is cooled by equilibration with surrounding rock and conductive heat transfer to the overlying and underlying rock units. The model discussed in this paper is most applicable to thin aquifers as vertical temperature variations in the aquifer are not considered.

A semi-analytic model has been developed to calculate the temperature distribution of the system as a function of the flowrate into the aquifer, the temperature of the water entering the aquifer, initial linear temperature profile, system geometry, rock properties, and time (Bodvarsson et al., 1981). The primary assumptions are listed below:

- (1) The mass flow is steady in the aquifer, horizontal conduction is neglected, and temperature is uniform in the vertical direction (thin aquifer). Thermal equilibrium between the fluid and the solids is instantaneous.
- (2) The rock matrix above and below the aquifer is impermeable. Horizontal conduction in the rock matrix is neglected.
- (3) The energy resistance at the contact between the aquifer and the rock matrix is negligible (infinite heat transfer coefficient).
- (4) The thermal properties of the formations above and below the aquifer may be different, but all thermal parameters of the liquid and the rocks are constant.

The differential equation governing the temperature in the aquifer at any time (t) can be readily derived by performing an energy balance on a control volume in the aquifer:

$$\begin{aligned}
 z = 0: \quad & \left. \frac{\lambda_1}{b} \frac{\partial T_1}{\partial z} \right|_{z=0} - \left. \frac{\lambda_2}{b} \frac{\partial T_2}{\partial z} \right|_{z=0} \\
 & - \frac{\rho_w c_w q}{b} \frac{\partial T_a}{\partial x} - \frac{\rho_a c_a}{a} \frac{\partial T_a}{\partial t} = 0
 \end{aligned} \tag{1}$$

The **symbols** are defined in the nomenclature. In the caprock and the bedrock the one-dimensional heat-conduction equation controls the temperature:

$$z > 0: \quad 1 \frac{\partial^2 T_1}{\partial z^2} = \rho_1 c_1 \frac{\partial T_1}{\partial t} \quad (2)$$

$$z < 0: \quad 2 \frac{\partial^2 T_2}{\partial z^2} = \rho_2 c_2 \frac{\partial T_2}{\partial t} \quad (3)$$

The initial conditions are:

$$T_a(x, 0) = T_1(x, z, 0) = T_2(x, z, 0) \\ = T_{b1} - a(z - D) \quad (4)$$

The boundary conditions are:

$$T_a(0, t) = T_f, \quad t > 0 \quad (5a)$$

$$T_a(x, t) = T_1(x, 0, t) = T_2(x, 0, t) \quad (5b)$$

$$T_1(x, D, t) = T_{b1} \quad (5c)$$

$$T_2(x, -H, t) = T_{b2} = T_{b1} + a(H + D) \quad (5d)$$

The following dimensionless parameters are introduced:

$$\xi = \frac{\lambda_1 x}{\rho_w c_w q D}; \quad \tau = \frac{\lambda_1 t}{\rho_1 c_1 D^2} \quad (6a, b)$$

$$\theta = \frac{b}{D} \frac{\rho_a c_a}{\rho_1 c_1}; \quad \eta = \frac{z}{D} \quad (6c, d)$$

$$\gamma = \frac{\rho_2 c_2}{\rho_1 c_1}; \quad \omega = \frac{\lambda_2}{\lambda_1} \quad (6e, f)$$

$$T_D = \frac{T - T_{b1}}{T_f - T_{b1}}; \quad T_g = \frac{aD}{T_f - T_{b1}} \quad (6g, h)$$

$$\alpha = H/D \quad (6i)$$

The solution of equations (1)-(3) can be easily obtained in the Laplace domain

(Bodvarsson, 1981).

$$\eta = 0: \quad \mu = \frac{1}{p} [1 - T_g] \exp \left[ - \left[ \theta p + \frac{\sqrt{p}}{\tanh \sqrt{p}} + \frac{\omega \sqrt{q}}{\tanh \sqrt{q}} \right] + \frac{T_g}{p} \right]. \quad (7)$$

$$\eta > 0: \quad v = \frac{[u - T_g/p]}{\tanh \sqrt{p}} \eta \cosh \sqrt{p} - \frac{T_g}{p} (\eta - 1) \quad (8)$$

$$\eta < 0: \quad w = \frac{[u - T_g/p]}{\tanh \sqrt{p}} \eta \cosh \sqrt{\omega} \sqrt{\frac{\gamma p}{\omega}} + \frac{T_g}{p} (\eta - 1) \quad (9)$$

$$+ \frac{[u - T_g/p]}{\tanh \sqrt{\omega}} \eta \sinh \sqrt{\frac{\gamma p}{\omega}} - \frac{T_g}{p} (\eta - 1) \quad (9)$$

In equations (7)-(9),  $u$ ,  $v$ , and  $w$  represent the temperature, in the Laplace domain of the aquifer, the rock above the aquifer, and the rock below the aquifer, respectively. As equations (7)-(9) cannot easily be inverted from the Laplace domain, a numerical inverter was used to evaluate the equations.

Using this model, the evolution of these systems can be studied. In Figure 3, the evolution of a hypothetical system is shown. The dimensionless coordinates used are defined in equations (6a-6i). In simple terms, the graph can be envisioned as the evolution of a single temperature profile, at a given location ( $\xi$ ) away from the fault. Before the incidence of hydrothermal circulation, the temperature profile is linear (normal geothermal gradient). When water begins to flow up the fault and into the aquifer, the aquifer begins to heat up. The fluid flows laterally in the aquifer, losing heat by conduction to the caprock and basement. A distinctive temperature reversal forms below the aquifer. With increasing time, conductive heat losses to the caprock stabilize and a typical linear conductive gradient is established. At very large times, the temperature below the aquifer stabilizes and for the case considered, becomes nearly constant with depth.

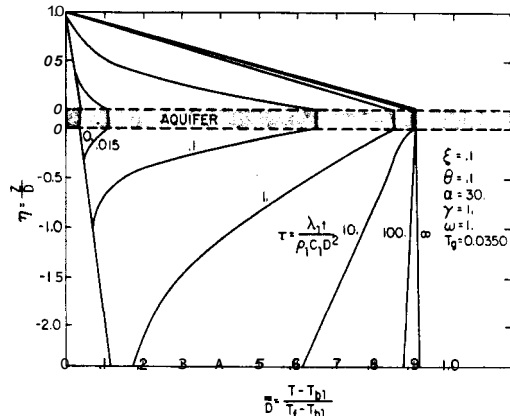
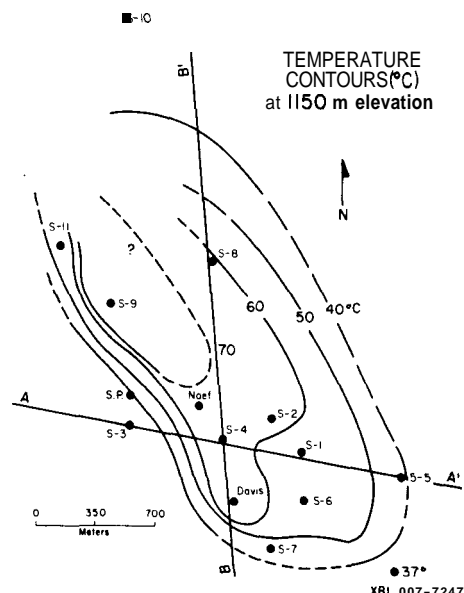


Figure 2 Evolution of a fault-charged hydrothermal system. This schematic represents the evolution of a single temperature profile over time.

Another application of this model is to calculate the rate of hot water recharge into an aquifer, given sufficient information about the areal and vertical temperature distribution in the aquifer. The model has been applied to the Susanville, California hydrothermal system, a low-temperature system located in the foothills of the Sierra Nevada. Data from more than twenty shallow exploration and production wells have outlined a thermal anomaly which is elongated around a north-west trending axis (Benson et al., 1980). Temperature contours at a depth of approximately 125 m below the surface (elevation 1150 m) are shown in Figure 3. Temperature profiles from several of the wells are shown in Figure 4. In each well temperatures increase linearly with depth until approximately 125 m below the surface. Thereafter the temperatures remain isothermal or have a reversal. The shape of the thermal anomaly can be explained by a recharging fault, which is slightly to the east of Suzy 9 and aligned with the northwest trend of the anomaly. The match of calculated and observed temperatures shown in Figure 4 was obtained by assuming a hot water recharge rate ( $80^{\circ}\text{C}$ ) of  $9 \times 10^{-6} \text{ m}^3/\text{sec/m}$  (obtained by trial and error) along the length of the fault. The remaining parameters used to obtain this match are shown in Table 1. Temperature contours were also considered for the match of the calculated and observed temperature distribution. A match using the same recharge rate ( $9 \times 10^{-6} \text{ m}^3/\text{sec/m}$ ) and recharge temperature ( $80^{\circ}\text{C}$ ) is shown in Figure 5. The match of observed and calculated values is very good close to the recharging fault. However, further from the fault the match is not very good. The discrepancy could be due to any number of factors: the regional flow of cold water from the north-west, complexity of the geologic



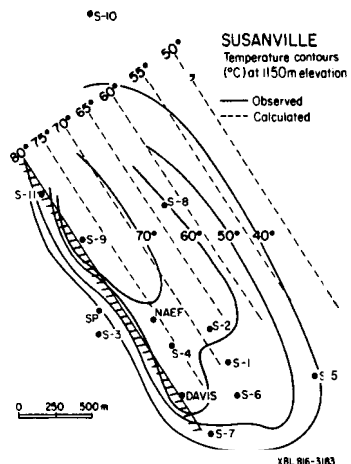


Figure 5 Match of calculated and observed temperature contours at Susanville.

used: maintenance of sufficiently high production temperature. Because the system is highly non-isothermal, and transient thermal phenomena are important, a numerical simulator was used to model the response of a fault-charged reservoir to pressure transient testing and sustained production from a well.

The recently developed numerical simulator PT (Pressure-Temperature) was used. The simulator solves the mass and energy transport equations for a liquid saturated heterogeneous porous and/or fractured media. The model includes the temperature dependence of fluid density, viscosity, and expansivity. It employs the integrated finite difference method for discretizing the medium and formulating the governing equations. The set of linear equations arising at each timestep are solved by direct means, using an efficient sparse solver. A detailed description of the simulator is given by Bodvarsson (1981).

To demonstrate the application of a numerical simulator to a fault-charged reservoir, the Susanville hydrothermal system was modeled. The geometry of the system was determined by correlation of well logs, drill cuttings and temperature profiles. Whereas the system is highly complex, we used a simplified model of the system which accounts for the major hydrothermal features. A cross section of the reservoir model and confining strata is shown in Figure 6. A 35 m-thick aquifer with a permeability of 2 Darcies is overlain by an impermeable caprock and underlain by a 240 m-thick impermeable bedrock. The ground surface temperature is a constant 10°C. The temperature at the bottom of the section (400 m depth) is a constant 22°C. To determine the temperature everywhere else in the system, the analytic solution discussed in the previous section was used, incorporating a recharge rate of  $9 \times 10^{-6} \text{ m}^3/\text{sec}/\text{m}$  (at 80°C).

This temperature distribution is close to the measured temperature distribution.

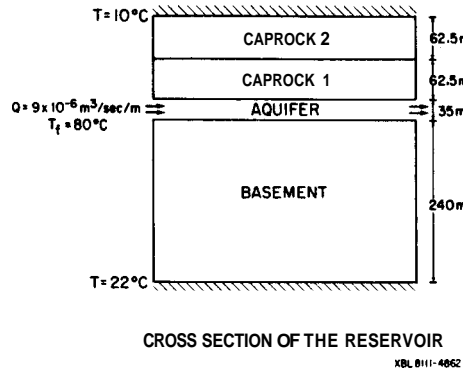


Figure 6 Cross section of the reservoir model used for numerical simulation of the Susanville hydrothermal system showing the four layers used in the mesh, the boundary conditions, and aquifer location.

The initial temperature and pressure distribution in the aquifer as a function of distance from the fault are shown in Figure 7. The pressure distribution in the aquifer was calculated so that the fault would sustain a rate of  $9 \times 10^{-6} \text{ m}^3/\text{sec}$  per linear meter. As shown in Figure 7, the pressure gradient close to the fault is small compared to far from the fault, where it is approximately 17 psi/km. This is as expected because the fluid viscosity close to the fault is less than half the viscosity of the 20°C fluid far from the fault. Gravity was neglected in all of the simulations. A constant potential boundary condition was imposed at the downstream end of the system. At the fault, two different boundary conditions were imposed: constant potential and constant flow. The mesh used in the simulations is shown in Figure 8. Only one-half of the flow field is modeled, due to the symmetry in the problem.

Reservoir Longevity The first objective of this simulation was to determine the production temperature vs. time for a well located 600 m from the fault. The initial temperature at the production well was 60°C.

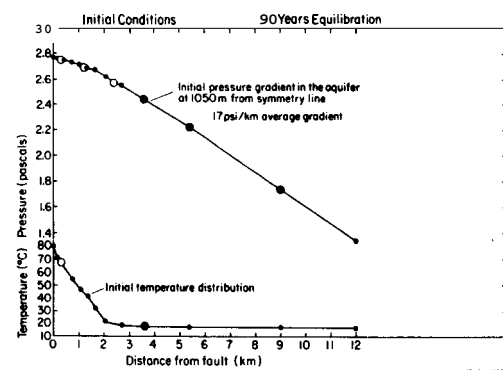


Figure 7 Initial pressure and temperature distribution in the aquifer.

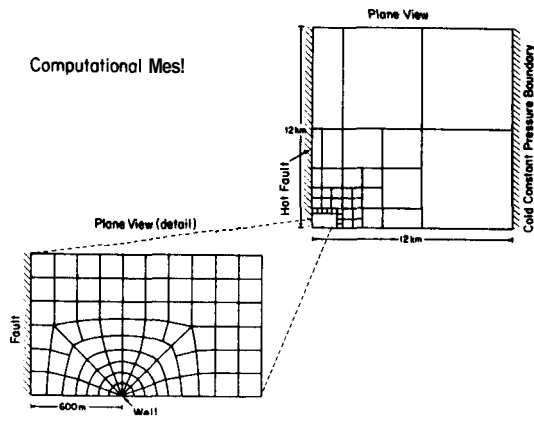


Figure 8 Plane view of the mesh used for the numerical simulations.

The well was then produced at a rate of 31 kg/sec (500 gpm). Figure 9 shows a plot of the production temperature over a 30-year lifetime for two cases: one with a constant potential fault and one in which the fault maintains a constant flow. As shown, the temperature in the constant flow rate case remained nearly constant during the 30-year lifetime. Only near the end of the period did the temperature begin to decline. Where the fault was at a constant potential, the temperature gradually increased with time and after the 30-year period the production temperature increased from 60°C to 67°C. This is readily explained by the increased rate of flow from the fault resulting from the production-induced drawdown near the fault. Figure 10 shows a plot of recharge rate vs. distance from the line of symmetry. Near the production well the recharge rate was nearly three times as great as the steady value which created the initial thermal anomaly. Temperature contours after 30 years of production are compared to the initial contours in Figure 11. As illustrated, the more mobile hot water moved quickly toward the production well causing the production temperature to increase. The cold water also moved toward the production well but at a slower rate.

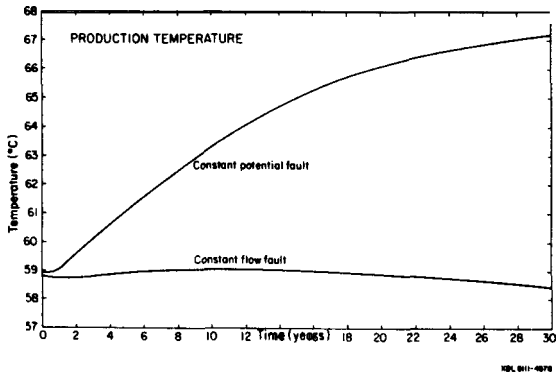


Figure 9 Production temperature vs. time for a well producing from a fault-charged reservoir for two cases: (1) a constant potential fault and (2) a constant flow fault.

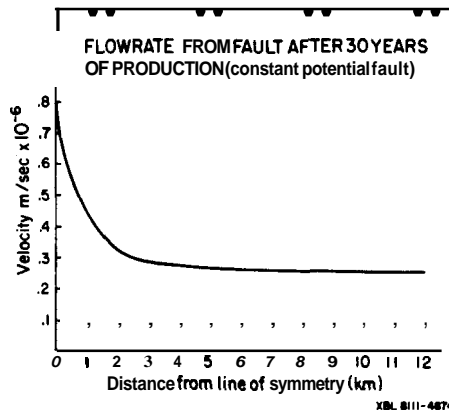


Figure 10 Flowrate from a constant potential fault near a well being produced at 31 kg/s (after 30 years of production).

This simulation demonstrates that for fault-charged hydrothermal systems, it is critical to include the recharge for an accurate reservoir assessment. If no recharge is considered then all of the hot water initially within the 60°C contour will be removed within ten years [at a rate of 31 kg/s (500 gpm)]. Both of the other cases (constant potential and constant flow) demonstrate that the resource will be adequate for a minimum of 30 years. The constant potential case suggests that the resource may be enhanced by exploitation. The nature of the recharging fault is clearly a key parameter to understanding and exploiting these systems.

Pressure Transient Analysis The same mesh and reservoir parameters were used to simulate a 30-day production/interference test in a fault charged reservoir. The production well was produced at a constant rate of 31 kg/s and pressure changes were observed in the production well and two interference wells. Analysis of the production well data gave a transmissivity of  $4.8 \times 10^5$  md·ft/cp, the value used in the simulation (corresponding to

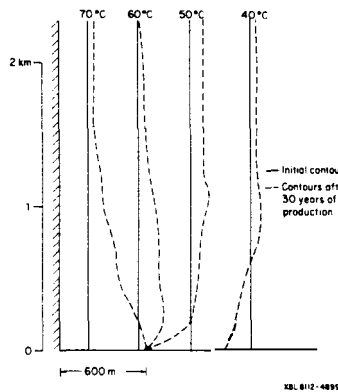


Figure 11 Comparison of temperature contours between their initial value and after 30 years of production from a well bounded by a constant potential fault.

the fluid viscosity at 60°C). Figure 12 shows a semi-log plot of the pressure transient data from the production well. As expected, the early time data falls on a straight line and later stabilizes, indicating a constant potential boundary. Figure 13 shows a schematic of the well locations, and the drawdowns at the observation wells for the constant potential fault case. At early times the drawdown at each well appears to follow the Theis curve, but later the drawdown falls below the Theis curve, indicating that the constant potential boundary is affecting the data. Type curve analyses were performed on both wells and transmissivities ( $kh/\mu$ ) of  $1.1 \times 10^6$  md·ft/cp and  $1.76 \times 10^6$  md·ft/cp were obtained. Because fluid viscosity changes by a factor of  $2^{1/2}$  in the temperature range considered, the highly non-isothermal temperature distribution and proximity to the "hot" fault obscure the normal pressure transient response. This effect of viscosity contrasts on non-isothermal well test analysis have been discussed previously (Mangold et al., 1981). This exercise seems to indicate that interference data may not provide data that can be accurately analyzed with standard methods. However, if sufficiently accurate early-time production data are available, a value for the reservoir transmissivity may be obtained and the nature of the fault may be determined. This type of pressure transient phenomena has been observed at the Susanville anomaly where analysis of production data gave a transmissivity value of  $7.3 \times 10^5$  md·ft/cp and several observation wells yielded transmissivities ranging from  $2.3 \times 10^6$  md·ft/cp to  $3.6 \times 10^6$  md·ft/cp.

#### Production and Reinjection Well Siting

Location of the production well as close as possible to the fault will allow production of the hottest fluid; this will also optimize the stimulation of recharge from a fault. Proper reinjection well siting is critical in fault-charged systems because an inappropriately placed reinjection well can create premature cooling of the production well. Reinjection well siting criteria are as follows:

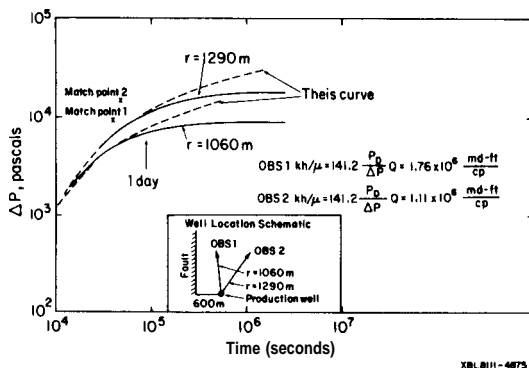


Figure 12 Drawdown and semi-log analysis of data from a production well in a reservoir bounded by a constant potential fault.

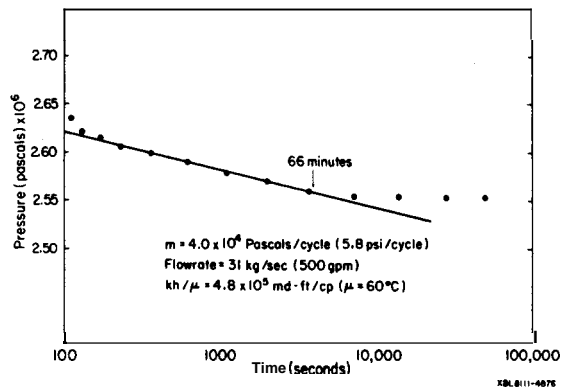


Figure 13 Drawdown and type curve analysis for the interference wells in an aquifer bounded by a constant potential fault.

(1) One should reinject downstream from the production well.

(2) If a constant potential fault is present, care should be taken to locate the reinjection well so that the pressure buildup due to reinjection does not negate the production-enhanced flow from the fault. If the aquifer is sufficiently permeable (pressure support not needed), and the produced fluids can be disposed of by some means other than reinjection, it may be desirable not to reinject or to reinject far from both the production well and the fault.

(3) The steady-state interflow between the production and injection well should be minimized. With proper siting, interflow between the wells may be negligible in an aquifer with regional flow (Dacosta and Bennett, 1960).

**Conclusion** By using a newly developed computational model for fault-charged reservoirs and a numerical simulator (PT), the effects of hot-water recharge into a near-surface hydrothermal aquifer have been included in reservoir engineering calculations. Key system parameters have been identified, the most important being the hydrologic characteristics of the fault itself. More simply, the ability of the fault to continue to provide hot water under production-induced reservoir conditions is critical to the longevity of the system. Two different boundary conditions for the fault have been investigated: a constant potential and a constant flow boundary. The constant flow case can be considered as a conservative case and the constant potential case as optimistic.

The methodology discussed in this paper has been applied to the Susanville, California hydrothermal resource. Predictions have been made of how the temperature will change with time, given a simple exploitation strategy.

Lifetime estimates and reservoir assessment using the methodology discussed herein are considerably more optimistic than those made if the hot water recharge into the system is ignored.

#### Nomenclature

a	= Geothermal gradient ( $^{\circ}\text{C}/\text{m}$ )
b	= Aquifer thickness (m)
c	= Heat capacity ( $\text{J}/\text{kg} \cdot ^{\circ}\text{C}$ )
D	= Thickness of caprock (m)
H	= Thickness of bedrock (m)
k	= Permeability ( $\text{md}, 10^{-15} \text{ m}^2$ )
p	= Laplace parameter
$\phi$	= Porosity
q	= Fault recharge rate ( $\text{m}^3/\text{s} \cdot \text{m}$ )
Q	= Well flow rate (kg/s)
t	= Time (sec)
T	= Temperature ( $^{\circ}\text{C}$ )
$T_{b1}$	= Temperature at ground surface ( $^{\circ}\text{C}$ )
$T_f$	= Temperature of recharge water ( $^{\circ}\text{C}$ )
u	= Temperature in aquifer in Laplace domain
v	= Temperature in rock matrix above aquifer in Laplace domain
w	= Temperature in rock matrix below aquifer in Laplace domain
x	= Lateral coordinate (m)
z	= Vertical coordinate (m)
$\lambda$	= Thermal conductivity ( $\text{J}/\text{m} \cdot \text{s} \cdot ^{\circ}\text{C}$ )
$c_p$	= Volumetric heat capacity ( $\text{J}/\text{m}^3 \cdot ^{\circ}\text{C}$ )
$\mu$	= Viscosity ( $\text{cp}, 10^{-3} \text{ Pa} \cdot \text{s}$ )

#### Subscripts

a	= Aquifer
1	= Rock matrix above aquifer
2	= Rock matrix below aquifer
w	= Liquid water

Acknowledgments This work was supported by the Assistant Secretary for Conservation and Renewable Energy, Office of Renewable Technology, Division of Geothermal and Hydropower Technologies of the U.S. Department of Energy under Contract No. W-7405-ENG-48.

#### References

Benson, S.M., Goranson, C.B., Noble, J., Schroeder, R.C., Corrigan, D., and Wollenberg, H. (1980), "Evaluation of the Susanville, California Geothermal Resource," Lawrence Berkeley Laboratory, Berkeley, California, LBL-11187.

Bodvarsson, G.S. (1981), "Mathematical Modeling of the Behavior of Geothermal Systems Under Exploitation," (Ph.D. dissertation) Lawrence Berkeley Laboratory, Berkeley, California.

Bodvarsson, G.S., Miller, C.W., and Benson, S.M. (1981), "A Simple Model for Fault-Charged Hydrothermal Systems," Lawrence Berkeley Laboratory, Berkeley, California, LBL-12869. Also presented at the Geothermal Resources Council Annual Meeting, 1981, Texas.

DaCosta, J.A., and Bennet, R.R. (1960). "The Pattern of Flow in the Vicinity of a Recharging and Discharging Pair of Wells in an Aquifer Having Areal Parallel Flow," Int. Ass. Sci. Hydrol. Publ. 52, Commission of Subterranean Waters, p. 524-536.

Mangold, D.C., Tsang, C.F., Lippmann, M.J., and Witherspoon, P.A. (1981), "A Study of Thermal Discontinuity in Well Test Analysis," Journal of Petroleum Technology, v. 33, n. 6 (June) ■